

AU Grinstead W C; Rodgers G P; Mazur W; French B A; Cromeens D; Van Pelt C;
West S M; Raizner A E

CS Department of Medicine, Baylor College of Medicine, Houston, Texas..

SO CORONARY ARTERY DISEASE, (1994 May) 5 (5) 425-34.

Journal code: BYW. ISSN: 0954-6928.

CY United States

DT Journal; Article; (JOURNAL ARTICLE)

LA English

FS Priority Journals

EM 199501

Thank you,
Mojdeh Bahar
AU 1617

2/3/9

12/29

Admiral only

ADONIS - Electronic Journal Services

Requested by

Adonis

Article title	Comparison of three porcine restenosis models: the relative importance of hypercholesterolemia, endothelial abrasion, and stenting
Article identifier	095469289410035U
Authors	Grinstead_W_C Rodgers_G_P Mazur_W French_B_A Cromeens_D Van_Pelt_C West_S_M Raizner_A_E
Journal title	Coronary Artery Disease
ISSN	0954-6928
Publisher	Lippincott Williams and Wilkins
Year of publication	1994
Volume	5
Issue	5
Supplement	0
Page range	425-434
Number of pages	10
User name	Adonis
Cost centre	Development
PCC	\$20.00
Date and time	Friday, December 29, 2000 2:58:24 PM

Copyright © 1991-1999 ADONIS and/or licensors.

The use of this system and its contents is restricted to the terms and conditions laid down in the Journal Delivery and User Agreement. Whilst the information contained on each CD-ROM has been obtained from sources believed to be reliable, no liability shall attach to ADONIS or the publisher in respect of any of its contents or in respect of any use of the system.

THERAPY AND PREVENTION

Comparison of three porcine restenosis models: the relative importance of hypercholesterolemia, endothelial abrasion, and stenting

W. Carter Grinstead, George P. Rodgers, Wojciech Mazur,
Brent A. French, Douglas Cromeens, Carolyn Van Pelt,
Stewart M. West, and Albert E. Raizner

Background: Porcine models of post-angioplasty restenosis commonly rely on hypercholesterolemia, endothelial abrasion, and intracoronary stenting to induce neointimal thickening. Although stenting clearly induces marked thickening, the influence of pre-stenting endothelial abrasion, and pre- and post-stenting hypercholesterolemia, on the degree and nature of post-stenting neointimal thickening is not clear. In order to assess this influence, we compared the quantity and quality of neointimal thickening in three stented swine restenosis models.

Methods: Twenty-three Hanford miniature swine completed one of three protocols. Model A animals (n=9) were fed a cholesterol-raising diet, underwent endothelial abrasion of the left anterior descending (LAD) and circumflex (CFX) coronary arteries after 2 weeks on this diet, had balloon-expandable tantalum coil stents placed in the right coronary artery (RCA), LAD, and CFX after 9 weeks on the diet, and were killed 4 weeks later (total of 13 weeks on diet). Model B animals (n=7) were also fed the cholesterol-raising diet, underwent stenting after 5 weeks on the diet, and were killed 4 weeks later (total of 9 weeks on diet). Model C animals (n=7) were fed normal swine food, underwent stenting, and were killed 4 weeks later. Endothelial abrasion was not performed in models B and C.

Results: Quantitative angiography revealed no significant differences between models in the change of minimal lumen diameter (mm±SD) of stented vessels from post-stenting to pre-sacrifice (LAD: 1.05 ± 0.74 , 0.75 ± 0.62 and 1.05 ± 0.34 ; CFX: 1.00 ± 0.65 , 0.83 ± 0.51 and 1.17 ± 0.38 ; RCA: 0.99 ± 0.35 , 0.20 ± 0.34 , and 0.94 ± 0.80 for models A, B, and C, respectively; all $P = NS$). Likewise, morphometric analysis showed no differences in percentage area stenosis (%±SD) over the same time (LAD: 55 ± 15 , 44 ± 24 , and 42 ± 16 ; CFX: 54 ± 12 , 55 ± 17 , and 40 ± 15 ; RCA: 39 ± 20 , 34 ± 11 , and 26 ± 13 for models A, B, and C, respectively; $P = NS$). The neointima in each model predominantly consisted of smooth muscle cells and collagen matrix.

Conclusions: The degree and nature of coronary artery neointimal thickening 4 weeks after stenting in normolipemic swine are similar to those in stented swine after 9 weeks on a high-cholesterol diet or 13 weeks on a high-cholesterol diet and early endothelial abrasion. The insertion of an intracoronary stent appears to be the major stimulus to neointimal thickening in these swine models of post-angioplasty restenosis.

Coronary Artery Disease 1994, 5:425-434

Keywords: angioplasty, swine, atherosclerosis

Restenosis remains the primary problem limiting the long-term success of percutaneous transluminal

coronary angioplasty. To date, no pharmacologic or mechanical method has consistently prevented

From the Department of Medicine, Section of Cardiology, Baylor College of Medicine and The Methodist Hospital, Houston, Texas, USA.

Sponsorship: Supported by a grant from the American Heart Association Texas Affiliate and the Methodist Hospital Cardiac Catheterization Laboratories Research Fund.

Requests for reprints to Dr Albert E. Raizner, The Methodist Hospital, 8535 Fannin, MS F-1000, Houston, TX 77030, USA.

Date of receipt: 17 January 1994; accepted 18 March 1994.

restenosis. Since large clinical trials are expensive and time-consuming, experimental models that can efficiently test promising therapies are vital.

The porcine model offers the advantage of a coronary anatomy similar to that of humans and one suitable for intracoronary interventions [1]. Furthermore, swine are susceptible to spontaneous and diet-induced atherosclerotic lesions in many respects mimicking those in humans [2,3].

We [4-6] and others [7-9] have developed porcine models of restenosis that use balloon-expandable metallic stents to induce neointimal thickening. These models have variously used cholesterol-raising diets and pre-stenting balloon-induced coronary endothelial abrasion to augment this response. However, the incremental effect of hypercholesterolemia and pre-stenting endothelial abrasion over and above the stent-induced injury is not clear.

Therefore, in order to ascertain the relative contribution of endothelial abrasion and hypercholesterolemia, we compared the degree and nature of neointimal thickening in three porcine models, in all of which intracoronary stenting was used.

Methods

Animal preparation

Hanford miniature swine (15-25 kg) were obtained from a licensed laboratory animal supplier. All procedures and handling were performed in a way that minimized the discomfort of the animals. The guidelines of the American Physiological Society were followed closely. The protocol was approved by the Institutional Animal Care Use Committees at Baylor College of Medicine and the University of Texas MD Anderson Hospital (Houston, Texas, USA). The animals were entered into one of three experimental protocols, designated models A, B, and C. Table 1 illustrates the major differences between these models.

Model A: Prolonged hypercholesterolemia, endothelial abrasion, and stenting

Swine were fed an atherogenic diet, 2% of which was cholesterol, 15% fat, and 1.5% sodium cholate. The animals received 2-3% of their body weight of diet per day throughout the study.

Endothelial abrasion

Two weeks after beginning the diet, all model A animals underwent coronary endothelial abrasion. For 3 days before and 3 days after abrasion, the animals received 2-4 mg/kg of diltiazem orally three times per day and 80-160 mg aspirin orally per day. Sedation was achieved with 20 mg/kg ketamine, 0.1 mg/kg acepromazine, and 0.1 mg/kg atropine intramuscularly, and general anesthesia maintained with 1-5% halothane and oxygen via a standard 7-8 F endotracheal tube. Nifedipine (10 mg) was given buccally after intubation. The left carotid artery was isolated and an 8 F hemostatic sheath (USCI) inserted. The animals then received intravenous 200 U/kg heparin, 250 mg ampicillin, and 5 mg/kg bretylium tosylate. Additional bretylium was administered every 15 min. The left coronary artery was cannulated with a 7 F hockey stick or 6 F Judkins catheter. Intracoronary nitroglycerin (200-400 µg) was administered and angiography was performed. An appropriately sized 2.0-3.5 mm diameter balloon dilatation catheter (USCI Probe) was introduced into the left anterior descending (LAD) coronary artery via the guiding catheter. The balloon was inflated three times (30 s each; 2-4 atm) during which it was rapidly moved to and fro within the artery. The same procedure was repeated for the circumflex (CFX) artery. The right coronary artery (RCA) was not abraded, allowing comparison of the influence of abrasion on neointimal thickening between different arteries in model A. The catheter and sheath were then removed and the carotid artery ligated. The wound was repaired and the animals allowed to recover. Approximately 2.5 cm of 2% nitroglycerin paste was applied topically and 250-500 mg ampicillin was given orally three times daily for 5 days. The animals remained on the atherogenic diet

Table 1. Major features of the three experimental models.

	Model A	Model B	Model C
Number of animals	9	7	7
Diet/feeding duration	HC/13 weeks	HC/9 weeks	Normal/4 weeks
Abraded vessels*	LAD, CFX	None	None
Stented vessels	LAD, CFX, RCA	LAD, CFX, RCA	LAD, CFX, RCA
Sacrifice (after stenting)	4 weeks	4 weeks	4 weeks

*Abrasion performed 7 weeks before stenting. HC, high cholesterol; LAD, left anterior descending; RCA, right coronary artery; CFX, circumflex.

for the following 7 weeks and then underwent stent implantation.

Stent Implantation

The stents used were 2.0, 2.5, and 3.0 mm in diameter, 12 or 20 mm long, and were composed of a balloon-mounted tantalum wire (0.006 inch diameter) arrayed in an incomplete serpentine coil manner (Gianturco-Roubin Flex-Stent™, Cook Inc., Bloomington, Indiana, USA). The pre-, intra-, and postoperative medication regimens for the abrasion step were repeated for the stenting procedure. The right femoral artery was isolated, an arterial sheath inserted, and blood drawn for serum total cholesterol, high-density lipoprotein (HDL) cholesterol, and triglyceride levels. The left coronary system was then cannulated with an 8 F guide catheter. Intracoronary nitroglycerin (200–400 µg) was administered and coronary cineangiograms were obtained in 40° left and right anterior oblique projections. Previous work in our laboratory [4–6] showed that matching or only slightly oversizing (≤20%) stent diameter to lumen diameter results in marked neointimal thickening. Therefore, an appropriately sized to slightly oversized stent was implanted in the LAD by balloon inflation to 9 atm for 25 s. The balloon catheter was deflated and withdrawn, 200–400 µg intracoronary nitroglycerin administered, and coronary arteriography repeated. Additional doses of nitroglycerin, nifedipine, or both, were given if significant coronary spasm was observed. The CFX and RCA were stented using the same protocol. The catheter and sheath were removed, the femoral artery ligated, and the incision closed. Animals were then allowed to recover. The atherogenic diet was continued for the following 4 weeks, whereupon final angiography was performed and the animals killed.

Follow-up angiography and sacrifice

The pre and intra-operative medication regimens used for abrasion and stenting were repeated for the follow-up angiography. The right carotid artery was isolated and cannulated, then blood was drawn for serum total and HDL cholesterol and triglyceride levels. The left coronary system was cannulated with a 6 or 7 F catheter, intracoronary nitroglycerin administered, and 40° left and right anterior oblique angiograms recorded. Angiography of the RCA was performed in the same manner.

Immediately after the final angiogram, the animals were placed under deep general anesthesia. A left thoracotomy was performed and the aortic arch vessels ligated. The descending aorta was cannulated with a 7 F introducer and 0.1 mmol/l sodium cacodylate (pH 7.4) buffer was perfused into the ascending thoracic aorta and coronary arteries to a pressure of 100 mmHg. The pulmonary artery trunk was excised to exsanguinate the animal soon after the

buffer infusion was begun. The descending thoracic aorta was simultaneously cross-clamped. When the buffer had infused for 10 min, the coronary arteries were perfusion-fixed at 100 mmHg with modified Karnovsky's fixation [Polyscientific, Bayshore, New York, USA; 2.5% glutaraldehyde buffered with 0.1 mmol/l cacodylate (pH 7.4)] for 10–20 min. The coronary arteries, including the stented segments, were then dissected free from the underlying muscle and placed in 2.5% glutaraldehyde fixative.

Model B: Short-duration hypercholesterolemia and stenting

Animals were fed the atherogenic diet for 5 weeks, and then each animal underwent stenting of the LAD, CFX, and RCA in a manner identical to that of model A. The atherogenic diet was continued until final angiography and sacrifice 4 weeks after stenting. In contrast to model A, no endothelial abrasion was performed and the total duration of feeding was 9 instead of 13 weeks.

Model C: Normal swine feed and stenting

Animals that had been given a normal non-atherogenic swine diet underwent stenting of the LAD, CFX, and RCA in a manner identical to that described for models A and B. Normal swine feed (Purina Mills) was continued for 4 weeks, angiography was performed, and the animals were killed. No endothelial abrasion was done.

Angiographic analysis and definitions

Immediate pre-stent, immediate post-stent, and pre-sacrifice angiograms of the LAD, CFX and RCA from each animal were analyzed with the computerized Cardiovascular Angiographic Analysis System. This system uses automated edge detection and correction for pincushion distortion. For a given animal, the projection that revealed the most severe narrowing before sacrifice was also analyzed for measurement before and after stenting. Minimal lumen diameter was measured at the narrowest site along the stented artery section. Percentage diameter stenosis was calculated as: $100 \times (1 - \text{minimal lumen diameter} / \text{proximal reference diameter})$. Mean lumen diameter was the mean of multiple vessel diameters measured throughout the length of the stented section. Change in minimal lumen diameter was the difference between immediate post-stent and pre-sacrifice minimal lumen diameter.

Morphometric analysis

The stented artery segments were cut into 3 mm sections and stent wires were carefully removed. Sections were paraffin-embedded, cut at a nomi-

nal thickness of 4 μ m, and stained with hematoxylin & eosin, Masson's trichrome, and Verhoeff-van Gieson stains. Slides were examined under light microscopy and the section of each artery with the most severely narrowed lumen underwent morphometric analysis with a projecting Olympus BH microscope ($\times 4$) with a drawing attachment. The borders of the internal elastic lamina (IEL) and vessel lumen were traced on a digitizing board. The areas bounded by the IEL (IEL area) and vessel lumen (luminal area) were calculated. On sections where the IEL was not completely intact, the IEL border was drawn at the division of neointima and normal media or adventitia. The percentage area stenosis was determined by: $100 \times (1 - \text{luminal area} / \text{IEL area})$. In addition, the maximal intimal thickness of each analyzed section was measured.

Histologic analysis

All vessels were evaluated for the presence and quantity of smooth muscle cells, fibrous connective tissue, foam cells, calcification, necrosis, macrophages, neutrophils, lymphocytes, eosinophils, and for disruption of the IEL and external elastic lamina (EEL). The following grading system was used to quantify each tissue component: 1, minimal, barely detectable; 2, mild, slightly detectable; 3, moderate, easily detectable; and 4, marked, very evident.

Endpoints

The primary angiographic endpoint was the change in minimal lumen diameter from post-stenting to pre-sacrifice, while secondary endpoints were pre-sacrifice percentage diameter stenosis, minimal lumen diameter, and mean lumen diameter. The primary morphometric endpoint was percentage area stenosis, whereas maximal intimal thickness was a secondary endpoint.

Statistical analysis

Angiographic, morphometric, and lipid measurements are given as means \pm SD for each of the models. Comparison between models A, B, and C was accomplished with an analysis of variance. The LAD, CFX, and RCA were analyzed separately. The paired Student's *t*-test was used to compare endpoints of the abraded LAD, abraded CFX, and unabraded RCA in model A. The nominal stent diameter (≤ 2.5 or 3.0 mm) of each artery in all three models was compared using the chi-squared test. Differences were considered significant when $P < 0.05$.

Results

Experimental course

Twenty-eight animals survived the protocol until stenting. Five animals died during stenting, three of ventricular fibrillation and two of bradycardia. No animal died after the stenting procedure. Therefore, 23 animals completed the study: nine, seven, and seven in models A, B, and C, respectively. All surviving animals had received LAD and RCA stents, but four CFX arteries were too small to stent (one, two, and one arteries in models A, B and C, respectively). Two pre-/post-stenting and two pre-sacrifice angiograms were technically unsuitable for quantitative analysis. All other angiograms and all tissue sections were adequate.

Lipid levels

Table 2 lists serum total cholesterol, HDL cholesterol, and triglycerides at stenting and pre-sacrifice for each model. At stenting, total and HDL cholesterol were greater in model A than in B and C, reflecting the 9 weeks of pre-stenting atherogenic feeding in model A compared with the 5 and 0 weeks in models B and C, respectively. However, at sacrifice 4 weeks later, models A and B had comparably ele-

Table 2. Serum lipid levels.

	Model A (n=9)	Model B (n=7)	Model C (n=7)	Significance (P)
Stenting				
Total cholesterol (mg/dl)	303 \pm 112	172 \pm 27	91 \pm 12	<0.01*
HDL cholesterol (mg/dl)	78 \pm 14	54 \pm 14	44 \pm 9	0.0001*
Triglycerides (mg/dl)	21 \pm 9	18 \pm 12	25 \pm 16	NS
Pre-sacrifice				
Total cholesterol (mg/dl)	267 \pm 88	239 \pm 66	73 \pm 13	<0.01†
HDL cholesterol (mg/dl)	86 \pm 16	74 \pm 8	39 \pm 6	0.0001†
Triglycerides (mg/dl)	27 \pm 17	28 \pm 14	26 \pm 7	NS

*A versus B and C; †A and B versus C. HDL, high-density lipoprotein.

vated total and HDL cholesterol levels, while model C levels remained significantly lower, as expected.

Table 3. Pre- and post-stenting angiographic data.

	Model A (n=9)	Model B (n=7)	Model C (n=7)	Significance (P)
Immediately before stenting				
Minimal lumen diameter (mm)				
LAD	2.2±0.3	2.1±0.3	2.0±0.3	NS
CFX	2.0±0.4	1.9±0.4	2.1±0.5	NS
RCA	2.5±0.3	2.4±0.1	2.7±0.6	NS
Mean lumen diameter (mm)				
LAD	2.6±0.3	2.5±0.3	2.5±0.4	NS
CFX	2.4±0.4	2.4±0.3	2.5±0.4	NS
RCA	2.8±0.3	2.7±0.2	3.1±0.5	NS
Immediately after stenting				
Stent: artery ratio				
LAD	1.01±0.15	1.05±0.14	1.15±0.15	NS
CFX	1.06±0.13	1.17±0.11	1.13±0.25	NS
RCA	0.93±0.06	0.96±0.10	0.89±0.11	NS
Minimal lumen diameter (mm)				
LAD	2.7±0.1	2.4±0.2	2.6±0.3	0.06*
CFX	2.7±0.2	2.3±0.5	2.5±0.3	NS
RCA	2.9±0.3	2.5±0.3	3.2±0.5	0.03†
Mean lumen diameter (mm)				
LAD	3.2±0.1	2.8±0.2	3.2±0.4	0.03*
CFX	3.1±0.2	2.7±0.4	3.0±0.3	NS
RCA	3.3±0.3	3.0±0.3	3.6±0.5	0.02†

*A versus B; †B versus C. LAD, left anterior descending; CFX, circumflex; RCA, right coronary artery.

Pre- and post-stenting angiography

Angiographic data obtained immediately before and after stenting are listed in Table 3. Before stenting, the vessel dimensions of each model were comparable. The nominal stent diameter was the same in all models when dichotomized at ≤2.5 and 3.0 mm, and stent-to-mean lumen diameter (stent:artery) ratio suggested a similar degree of injury across models. It was of importance that the mean stent:artery ratio was >1.0 for the LAD and CFX arteries, implying a tendency slightly to oversize the stent, while the mean ratio was <1.0 for RCAs, suggesting stent undersizing. All mean ratios were, however, within 2 SD of 1.0. Post-stenting minimal lumen (and mean lumen) diameter was greater in model A versus B for LAD and C versus B for RCA.

Pre-sacrifice angiography

As shown in Table 4 and Fig. 1, there were no statistically significant differences between models for any of the angiographic parameters measured. Although the change in minimal lumen diameter of $-0.20±0.34$ mm for the RCA in model B seemed smaller than that of the other models, the differences were not significant.

Table 4. Pre-sacrifice angiographic data.

	Model A (n=9)	Model B (n=7)	Model C (n=7)	Significance (P)
Change in minimal lumen diameter (post-stent to pre-sacrifice, mm)				
LAD	-1.05±0.74	-0.75±0.62	-1.05±0.34	NS
CFX	-1.00±0.65	-0.83±0.51	-1.17±0.38	NS
RCA	-0.99±0.35	-0.20±0.34	-0.94±0.60	NS
Minimal lumen diameter (mm)				
LAD	1.7±0.6	1.7±0.4	1.5±0.2	NS
CFX	1.7±0.6	1.5±0.3	1.3±0.3	NS
RCA	1.9±0.4	2.2±0.2	2.2±0.6	NS
Diameter stenosis (%)				
LAD	44±17	42±9	44±7	NS
CFX	42±15	47±87	51±11	NS
RCA	34±9	24±9	31±14	NS
Mean lumen diameter (mm)				
LAD	2.2±0.5	2.3±0.4	2.1±0.3	NS
CFX	2.2±0.6	2.0±0.1	2.1±0.1	NS
RCA	2.5±0.5	2.8±0.3	2.9±0.6	NS

LAD, left anterior descending; CFX, circumflex; RCA, right coronary artery.

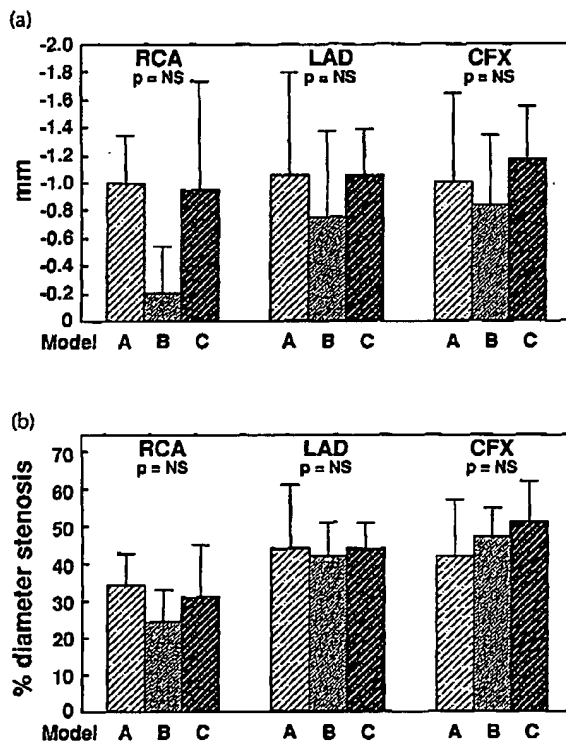


Fig. 1. Bar graphs showing mean (±SD) change in minimal lumen diameter from immediately after stenting to before sacrifice 4 weeks later (a) and angiographic percentage diameter stenosis immediately before sacrifice (b). RCA, right coronary artery; LAD, left anterior descending; CFX, circumflex.

Morphometric and histologic analyses

Percentage area stenosis and maximal intimal thickness were similar in all models (Table 5 and Fig. 2).

Table 5. Morphometric data.

	Model A (n=9)	Model B (n=7)	Model C (n=7)	Significance (P)
Area stenosis (%)				
LAD	55±15	44±24	42±16	NS
CFX	54±12	55±17	40±16	NS
RCA	39±20	34±11	26±13	NS
Maximal intimal thickness (μm)				
LAD	680±186	498±167	619±158	NS
CFX	620±233	719±284	567±187	NS
RCA	517±244	526±278	479±147	NS

LAD, left anterior descending; CFX, circumflex; RCA, right coronary artery.

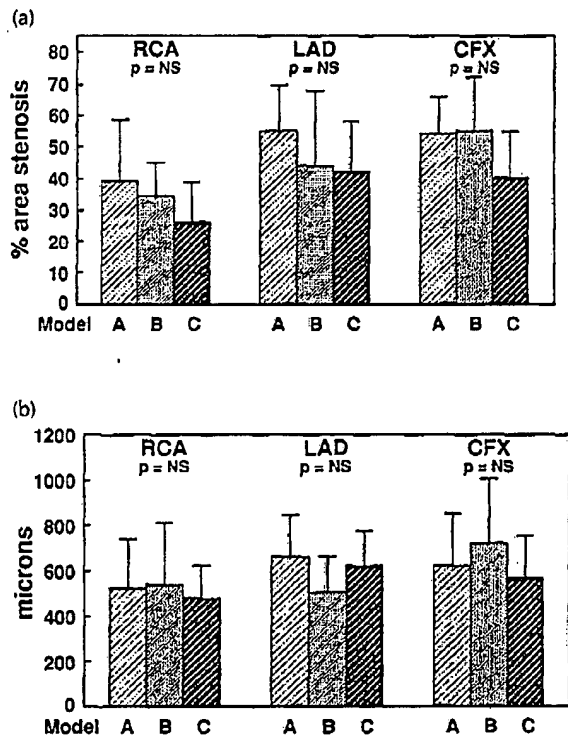


Fig. 2. Bar graphs showing mean (±SD) morphometric percentage area stenosis (a) and maximal intimal thickness (b). RCA, right coronary artery; LAD, left anterior descending; CFX, circumflex.

Histologic analysis revealed a similar degree of vessel injury in each model. In all stented vessels, the IEL was clearly disrupted, primarily at the stent wire sites. In addition, the EEL was disrupted in 25 out of 26 model A vessels, 17 out of 18 model B vessels, and 15 out of 19 model C vessels. Of the vessels without EEL disruption three were RCA and one LAD in model C, and one RCA in each of models A and B. Five of these six vessels with intact EEL were RCA,

a finding consistent with the relatively lower RCA stent:artery ratios noted on angiography.

The response to injury in each model was essentially identical (Fig. 3). Each model produced significant and similar neointimal thickening primarily consisting of smooth muscle cells and fibrous connective tissue, although the extent of this response varied within each group. No calcification was observed. Foam cells were present minimally in three model A and one model B animals, but were not present in model C animals. Table 6 shows mean severity grades for each tissue component.

In all models, the stent struts frequently extended into the adventitia and were associated with focal necrosis, sporadic hemorrhage, fibrous connective tissue deposition, and a mixed inflammatory reaction consisting of smooth muscle cells, multinuclear giant cells, lymphocytes, plasma cells, eosinophils, and mast cells. This inflammatory response surrounding stent sites suggests the possibility of a hypersensitivity reaction (Fig. 4).

Effect of endothelial abrasion in model A

The LAD and CFX arteries in model A underwent abrasion, whereas the RCAs did not. Table 7 compares the angiographic and morphometric endpoints of the abraded LAD and CFX and the unabraded RCA in model A. The RCA morphometric area stenosis of 39±20% was significantly different from the 55±15% for the LAD ($P<0.05$), but not statistically different from the 54±12% for the CFX ($P<0.10$). All other comparisons showed no differences between the arteries, implying that abrasion had little or no effect on intimal thickening.

Discussion

In this study we compared three strategies for inducing coronary artery neointimal thickening in swine. All three models used intracoronary stenting. Model A incorporated prolonged high-cholesterol feeding (13 weeks) and endothelial abrasion, a design similar to an effective model previously developed in our laboratory [4-6]. Model B tested the influence of a shorter high cholesterol feeding period (9 weeks) in animals not subjected to the risk and expense of an abrasion procedure. Model C was a streamlined protocol with no abrasion step and no special feeding requirement before stent insertion. Despite these protocol differences, no significant differences in angiographic, morphometric, and histologic endpoints were detected between the three models. This finding suggests that the primary impetus for neointimal thickening was stenting, and that hypercholesterolemia and abrasion played a less important role, which was overshadowed by the response to stent injury.

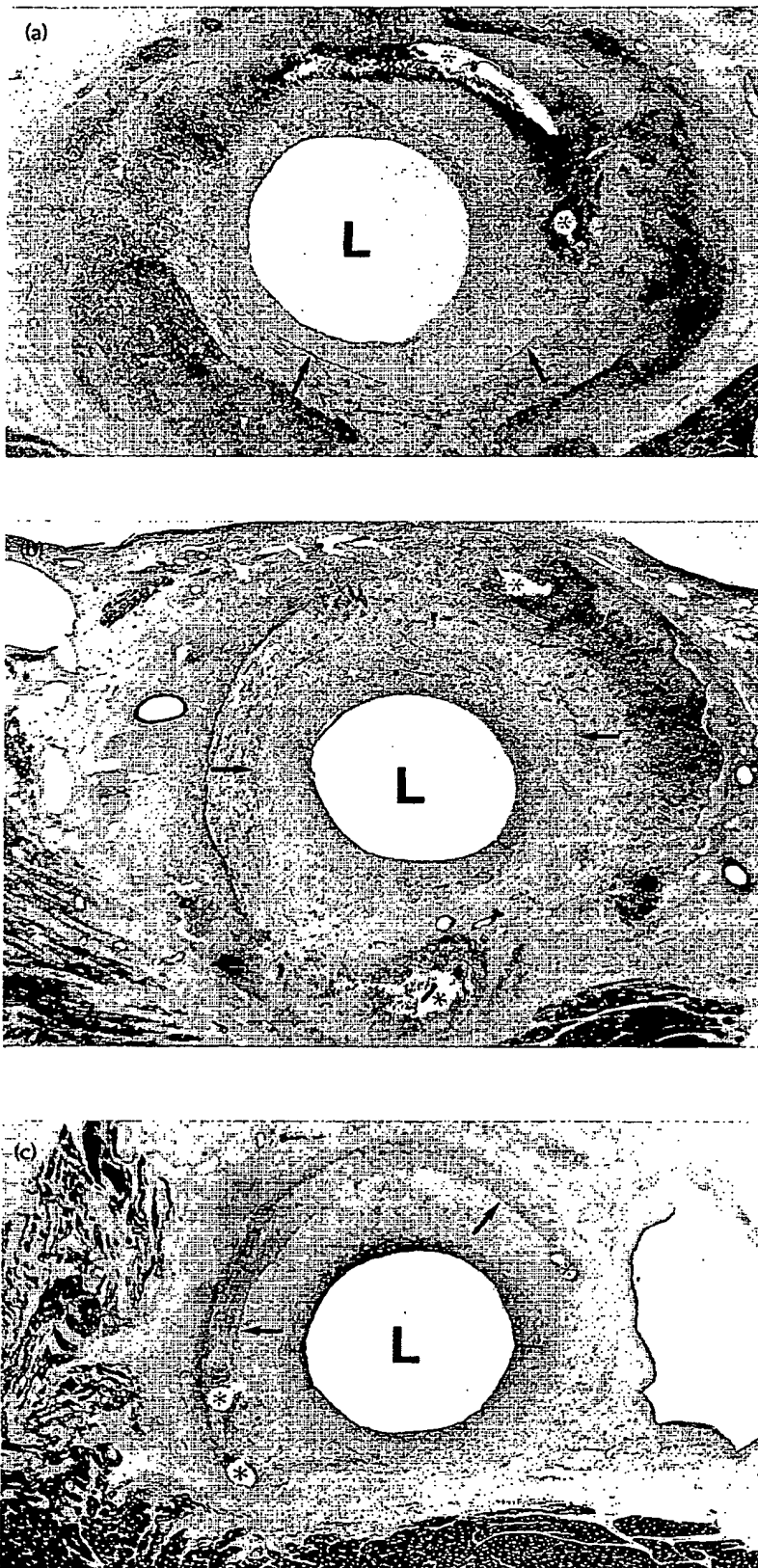


Fig. 3. Photomicrographs of stented left anterior descending arteries from models A, B and C; (a), (b) and (c), respectively. 'L' designates lumen, arrows point to the internal elastic lamina (IEL), and asterisks indicate the former locations of stent struts. Concentric neointimal thickening is present between the intact/disrupted IEL and lumen. Magnification: (a), ×30, (b) and (c), ×35.

Table 6. Mean histologic grades.

Vessel	Model	Smooth muscle cells	Fibrous connective tissue	Foam cells	Necrosis	Macrophages	Neutrophils	Lymphocytes	Eosinophils
LAD	A	3.7	2.9	0	1.3	1.6	1.6	2.8	2.0
	B	2.9	2.3	0	1.1	1.9	1.0	2.3	1.9
	C	2.7	2.7	0	0.7	1.1	0.6	1.6	0.9
CFX	A	3.4	3.0	0.3	1.3	2.3	1.4	2.9	2.1
	B	2.0	2.0	0.2	1.0	0.4	0.4	1.0	2.0
	C	2.8	2.8	0	0.8	1.0	0.6	2.0	1.0
RCA	A	3.1	3.0	0.1	1.4	1.4	1.3	2.9	1.7
	B	2.8	2.0	0	0.8	1.0	1.0	1.5	1.0
	C	2.1	2.1	0	1.3	0.6	0.1	1.0	0.7

LAD, left anterior descending; CFX, circumflex; RCA, right coronary artery.

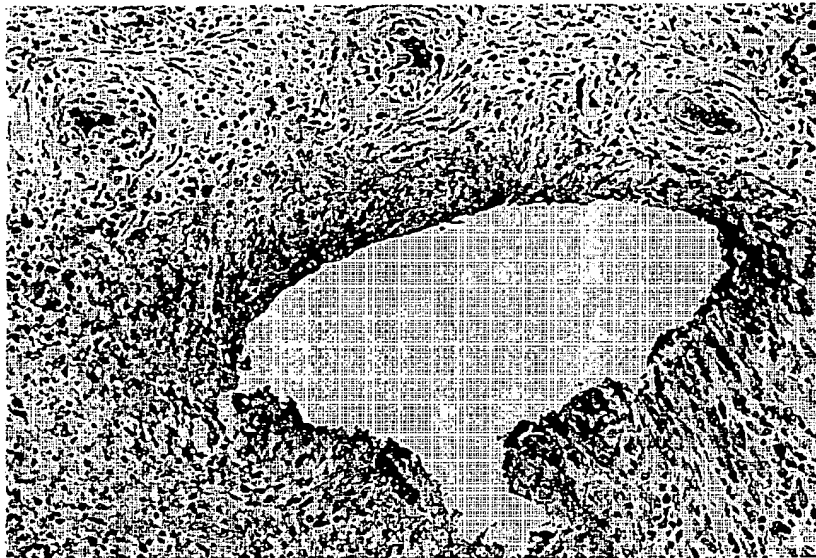


Fig. 4. Close-up photomicrograph of a stented circumflex artery from model A showing a cellular inflammatory reaction, including multinuclear giant cells, surrounding a stent strut site (stent removed). (Magnification: $\times 285$.)

Table 7. Effect of endothelial abrasion in model A.

	LAD* (n=9)	CFX* (n=9)	RCA† (n=9)	Significance (P)
Change in minimal lumen diameter (mm)	-1.05 ± 0.74	-1.00 ± 0.65	-0.99 ± 0.35	NS
Diameter stenosis (%)	44 ± 17	42 ± 15	34 ± 9	NS
Change in diameter stenosis (%)	36 ± 28	35 ± 24	31 ± 13	NS
Area stenosis (%)	55 ± 15	54 ± 12	39 ± 20	$<0.05^\ddagger$
Maximal intimal thickness (μm)	660 ± 186	620 ± 233	517 ± 244	NS

*Abrasion performed; †No abrasion performed. ‡Right coronary artery (RCA) versus left anterior descending (LAD). CFX, circumflex.

Histologic analysis revealed that stent insertion disrupted the IEL in all vessels and the EEL in all but six (10%). We attempted to maintain the nominal stent diameter: mean vessel diameter ratio at 1.0–1.2, and this was successful in that the angiographic mean stent:artery ratios ranged from 0.89 to 1.17. Extensive medial and adventitial injury occurred despite

the lack of marked stent oversizing, somewhat surprisingly. Nevertheless, this model of injury is relevant, since deep medial and adventitial tears can occur after angioplasty in humans [10].

The mean stent:artery ratio was <1.0 for the RCA in all models, but >1.0 for the LAD and CFX. Five of 22 RCAs, but only one of 41 LAD and CFX arteries, did

not exhibit EEL disruption. This slight oversizing of LAD and CFX stents and relatively more severe vessel injury may explain the trend towards a higher degree of stenosis in these vessels compared with the RCA. This finding is consistent with a recently proposed hypothesis correlating vessel injury with the degree of neointimal thickening [8].

A combination of cholesterol feeding and balloon-induced endothelial abrasion has been shown to accelerate atherosclerosis in the aorta [11], iliac [12], and coronary arteries [13] of swine. However, the relative importance of cholesterol feeding and endothelial injury in swine coronary atherosclerosis is unclear. In 11 animals on a high-cholesterol diet, Weiner *et al.* [14] balloon-abraded the LAD, but not the CFX or RCA. After 8 months, histologic analysis revealed similar disease in all three coronary arteries [14]. Likewise, Griggs *et al.* [15] reported a significant positive correlation between serum cholesterol and the extent of intimal lesions after 4 months of cholesterol feeding but no difference between balloon-injured and non-balloon-injured vessels. Our own study, in 21 hypercholesterolemic swine exposed to balloon dilatation of the RCA but not the CFX, resulted in 2-month follow-up angiographic diameter stenoses of 8 and 7%, respectively, a non-significant difference [15]. In contrast to these three studies, which all suggest a lesser role for endothelial injury, Schneider *et al.* [16] reported no difference in maximal intimal thickness and the ratio of luminal to intimal areas between swine exposed to overstretched balloon injury alone and swine exposed to balloon injury plus hypercholesterolemia (580 mg/dl), implying a less important role for cholesterol feeding.

Although the relative roles of dietary manipulation and endothelial abrasion are unclear, intracoronary stenting clearly induces predictable neointimal thickening in swine and is now the foundation for restenosis models in our laboratory [4–6] and at other institutions [7–9]. The Mayo Clinic model relies on oversizing a coil stent by 20–100% to produce stenoses of up to 100% (mean 63%) and does not include cholesterol feeding or a separate abrasion step [7,8]. Karas *et al.* [9] at Emory University recently reported a significantly greater degree of neointimal thickening after the placement of tantalum Wiktor stents (20–30% oversized) than with balloon injury alone in normolipemic swine. In our models, we achieved mean angiographic stenoses 4 weeks after stenting ranging from 24 to 51%, which may be a more clinically relevant response to injury than the severe stenoses observed in models using more aggressive stent oversizing.

An earlier swine model developed in our laboratory used endothelial abrasion and high cholesterol feeding for 6 months in addition to stenting [4]. The duration, personnel required, and expense of this protocol is relatively large compared with that of a model incorporating shorter durations of cholesterol feeding or no additional abrasion step. The present

study confirms that a stented swine model incorporating normal feeding (model C) induced neointimal thickening comparable with a stented model incorporating 9 weeks of cholesterol feeding (model B) or endothelial abrasion and 13 weeks of cholesterol feeding (model A). The cost of performing a 20-pig study in our laboratory using model A is currently US \$49 970, while the cost of using the same number of animals in models B and C is US\$38 523 and US\$26 841, respectively. These values do not include the cost of stents, which were kindly supplied by the manufacturer.

Limitations of the study

The number of animals in each model was small. Consequently, small differences in outcome variables may have been missed. Furthermore, total cholesterol levels at sacrifice were of the order of 200–400 mg/dl in models A and B, lower than the 400–600 mg/dl in our previous hypercholesterolemic models. Therefore, we cannot rule out the possibility that more extreme hypercholesterolemia produces an incremental increase in neointimal thickening in a stented swine model, as earlier results have suggested [5]. Extreme hypercholesterolemia may also produce a histologic response more similar to that in humans, such as foam cell development, as was minimally produced in our hypercholesterolemic models A and B.

In conclusion, insertion of intracoronary balloon-expandable coil stents in normolipemic Hanford miniature swine induces neointimal thickening comparable with that produced with endothelial abrasion, 13 weeks of hypercholesterolemia and stenting, or 9 weeks of hypercholesterolemia and stenting without the abrasion step. A swine model of restenosis that incorporates normal feeding followed by stenting should produce comparable neointimal thickening in a timely manner and may be a more cost-efficient model of post-angioplasty restenosis for use in future investigations.

Acknowledgements

The authors thank Daryl Schulz for assisting with the experiments, John Abukhalil for analyzing the angiograms, and Rob Geske for preparing the tissue sections. We also thank Cook Inc., for supplying the stents.

References

1. Hughes HC: Swine in cardiovascular research. *Lab Anim Sci* 1986, 36:348–350.
2. French JE, Jennings MA, Florey HW: Morphological studies on atherosclerosis in swine. *Ann NY Acad Sci* 1965, 127:780–794.
3. Kim DN, Lee KT, Schmee J, Thomas WA: Quantification of intimal cell masses and atherosclerotic lesions in

- coronary arteries of control and hyperlipidemic swine. *Atherosclerosis* 1984, 52:115-122.
4. Rodgers GP, Minor ST, Robinson K, Cromeens D, Woolbert SC, Stephens LC, et al.: Adjuvant therapy for intracoronary stents: Investigations in atherosclerotic swine. *Circulation* 1990, 82:560-569.
 5. Woolbert SC, Minor ST, Smith GS, Rodgers GP, Mims M, Guyton JR, et al.: Intracoronary stenting accelerates luminal narrowing in hypercholesterolemic swine. *Circulation* 1990, 82 (suppl III):III-656.
 6. Rodgers GP, Minor ST, Robinson K, Cromeens D, Stephens LC, Woolbert SC, et al.: The coronary artery response to balloon-expandable flexible stent in the aspirin and non-aspirin treated swine model. *Am Heart J* 1991, 122:640-647.
 7. Schwartz RS, Murphy JG, Edwards WD, Camrud AR, Vlietstra RE, Holmes DR: Restenosis after balloon angioplasty. A practical proliferative model in porcine coronary arteries. *Circulation* 1990, 82:2190-2200.
 8. Schwartz RS, Huber KC, Murphy JG, Edwards WD, Camrud AR, Vlietstra RD, et al.: Restenosis and the proportional neointimal response to coronary artery injury: results in a porcine model. *J Am Coll Cardiol* 1992, 19:267-274.
 9. Karas SP, Gravanis MB, Santoian ED, Robinson KA, Anderberg KA, King SB III: Endothelial intimal proliferation after balloon injury and stenting in swine: an animal model of restenosis. *J Am Coll Cardiol* 1992, 20:467-474.
 10. Nobuyoshi M, Kimura K, Ohishi H, Horiuchi H, Nosaka H, Hamasaki N, et al.: Restenosis after percutaneous transluminal coronary angioplasty: pathologic observations in 20 patients. *J Am Coll Cardiol* 1991, 17:433-439.
 11. Nam SC, Lee WM, Jarmolych J, Lee KT, Thomas WA: Rapid production of advanced atherosclerosis in swine by a combination of endothelial injury and cholesterol feeding. *Exp Mol Pathol* 1973, 18:369-379.
 12. Gal D, Rongione AJ, Slovenkai GA, DeJesus ST, Lucas A, Fields CD, et al.: Atherosclerotic Yucatan microswine: an animal model with high-grade fibrocalcific, nonfatty lesions suitable for testing catheter-based interventions. *Am Heart J* 1990, 119:291-300.
 13. Lee WM, Lee KT: Advanced coronary atherosclerosis in swine produced by combination of balloon catheter injury and cholesterol feeding. *Exp Mol Pathol* 1975, 23:491-499.
 14. Weiner BH, Ockene IS, Levine PH, Cuenoud HF, Fisher M, Johnson BF, et al.: Inhibition of atherosclerosis by cod-liver oil in a hyperlipidemic swine model. *N Engl J Med* 1986, 315:841-846.
 15. Griggs RT, Bauman RW, Reddick RL, Read MS, Koch GG, Lamb MA: Development of coronary atherosclerosis in swine with severe hypercholesterolemia. Lack of influence of von Willebrand factor or acute intimal injury. *Arteriosclerosis* 1986, 6:155-165.
 16. Schneider JE, Santoian EC, Gravanis MB, Cipolla G, Anderberg K, King SB III: Lovastatin fails to limit smooth muscle cell proliferation in normolipemic swine in an overstretch balloon injury model of restenosis. *J Am Coll Cardiol* 1992, 19:163A.